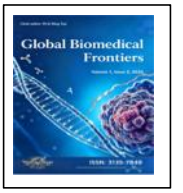
Global Biomedical Frontiers
https://www.vifpress.com/journals/global-biomedical-frontiers



In Pancreatic Cancer-Associated Fibroblasts under Conditions of Abundant Energy, the AMPK-ACC1 Signaling Pathway is Abnormally Activated

Leyi Zhang[1]*, Yunqi Ma[2]

[1] Beijing Veritas Prep School, Beijing, China
[2] Haidian Teacher Training School Affiliated Experimental School, Beijing, China

Information

Keywords：
pancreatic cancer;
cancer-associated fibroblasts;
AMPK;
ACC1;
metabolic reprogramming

Abstract

Pancreatic cancer is a highly malignant and poorly prognosed digestive tract tumor. In-depth study of the metabolic reprogramming of tumor-associated fibroblasts (CAF) in the tumor microenvironment is of great significance for researching molecular targets of drugs for treating pancreatic cancer. This experiment mainly compared CAF and normal fibroblasts (NF) to explore the activation mechanism of the AMPK-ACC1 signaling pathway in CAF under nutrient-rich conditions, providing a target for the treatment of pancreatic cancer. The experiment detected the transcriptional levels of AMPK and ACC1 in NF and CAF by qPCR, and the phosphorylation and non-phosphorylation levels of AMPK and ACC1 proteins in NF and CAF by Western Blot. The results showed that the mRNA contents of AMPK and ACC1 in CAF were higher than those in NF, and the protein expression contents of AMPK, ACC1, p-AMPK, and p-ACC1 in CAF were higher than those in NF. CAF activated AMPK phosphorylation and increased the transcriptional level of AMPK under a long-term high AMP/ATP ratio; ACC1 was highly expressed in CAF; AMPK promoted ACC1 phosphorylation, reduced the content of active ACC1, and decreased the level of fatty acid synthesis metabolism while increasing the level of fatty acid degradation metabolism, providing energy for CAF.

Introduction

Background

AMPK is a heterotrimeric complex composed of a catalytic α subunit and two regulatory subunits β and γ [1]. The cystathionine-β-synthase (CBS) domain of the γ subunit can simultaneously bind to AMP and ATP [2], sensing changes in the AMP/ATP ratio and phosphorylating the Thr172 site on the α subunit, activating AMPK and thereby regulating downstream molecules.

Acetyl-CoA carboxylase (ACC) is a key enzyme regulating fatty acid metabolism. Among them, ACC1 is located in the cytoplasm and catalyzes the generation of propionyl-CoA from acetyl-CoA, driving fatty acid synthesis [3]. In liver cancer cells, ACC1 is highly expressed [4]. Activation of AMPK leads to phosphorylation of the Ser79 site on ACC1, inhibiting enzyme activity [5], reducing the level of fatty acid synthesis metabolism. Activation of AMPK inhibits the transcription of ACC1, further inhibiting the synthetic metabolism [6-7].

Email: 1. Leyi Zhang*, yolandapeerz@gmail.com(Corresponding author); 2.Yunqi Ma, 13017670172@163.com.

Research Question and Experimental Design

AMPK is a hot topic molecule in recent years, but there have been no studies on it in pancreatic cancer-associated fibroblasts. This experiment explores the regulation of fatty acid metabolism by AMPK in pancreatic cancer-related fibroblasts to compensate for low ATP levels, involving its key energy source, affecting the activity of cancer-associated fibroblasts, and thereby should inhibit the proliferation, migration and invasion of pancreatic cancer cells, and can be used as a core target for pancreatic cancer treatment drugs.

1 Materials and Methods

1.1 Cells

Human pancreatic stellate cells (hPSCs), used as the NF comparison, and pancreatic CAFs were obtained from the Institute of Biophysics, Chinese Academy of Sciences. The abbreviations NF and CAF are retained in the figures to identify the two experimental groups.

1.2 Reagents

Table 1. Major experimental reagents.

Reagent	Manufacturer	Country/Region
Dulbecco's modified Eagle medium (DMEM)	Gibco	USA
Fetal bovine serum (FBS)	Hangzhou Sijiqing Biological Engineering Materials	China
Penicillin–streptomycin solution (100×); trypsin solution with phenol red; PBS; SDS-PAGE loading buffer (5×)	Biosharp	China
TRIzol reagent	Invitrogen	USA
Chloroform; absolute ethanol; isopropanol	Sinopharm Chemical Reagent (Hushi)	China
Absolute methanol	Beijing Beihua Fine Chemicals	China
Tween-20; bovine serum albumin (BSA-V)	Solarbio	China
Stain-free precast gels (4–12%)	Shanghai Epizyme Biomedical Technology	China
Enhanced chemiluminescence (ECL) reagent; 5× All-In-One RT Master Mix; PageRuler prestained protein ladder	Thermo Fisher Scientific	USA
Recombinant monoclonal antibodies to GAPDH, PRKAA1, phospho-PRKAA1, ACC1, and phospho-ACC1	Proteintech	China
Horseradish peroxidase-conjugated anti-rabbit secondary antibody	Cell Signaling Technology	USA
2× RealStar Power SYBR qPCR Mix	GenStar	China
Protease/phosphatase inhibitor cocktail (100×); RIPA lysis buffer	Beyotime Biotechnology	China

1.3 Instruments

Table 2. Major experimental instruments.

Instrument	Manufacturer	Country/Region
Thermal cycler; PowerPac Basic electrophoresis power supply	Bio-Rad Laboratories	USA

Instrument	Manufacturer	Country/Region
Microplate reader	Agilent	USA
Western blot imaging system	Shanghai Clinx Science Instruments	China
Centrifuge	Thermo Fisher Scientific	USA
Platform rocker	SCILOGEX	USA
Vortex mixer	WIGGENS	Germany
Constant-temperature water bath	Jintan Kexi Instrument	China
Shaking incubator	Harbin Donglian Electronic Technology Development	China
Rotor-Gene 6000 real-time PCR instrument	Corbett Research	Australia
NanoDrop microvolume spectrophotometer	NanoDrop	USA

1.4 Cell Culture

The NF and CAF cells were cultured in 100mm petri dishes using DMEM medium containing 10% FBS and 1% double anticoagulant (penicillin, streptomycin). The cells were placed in a cell culture incubator at 37°C and 5% CO2.

When the cells in the petri dish reached about 90% fullness, the cells were passaged. The original medium in the petri dish was discarded, 5mL PBS was added to wash away the residual FBS to prevent TE failure. 1mL TE was added under a microscope and when about 90% of the cells became round, 2mL DMEM (+/+) was added to deactivate TE. The medium in the petri dish was aspirated using a pipette and the adherent cells were shaken and transferred to a 15mL centrifuge tube. Centrifuge at 1000rpm for 3 minutes. After centrifugation, the supernatant was discarded and 1mL DMEM (+/+) was added to resuspend the cell precipitate. The cell suspension was added to a new petri dish and 10mL DMEM (+/+) was added to replenish, and then placed in the incubator for further culture.

1.5 RNA Extraction

When the cells in the petri dish have grown to more than 80% fullness, discard all the culture medium. Add 3 mL of DMEM (+/+) to dislodge the adherent cells on the petri dish and collect the cell suspension into a 15 mL centrifuge tube. Centrifuge at 1000 rpm for 1 minute, then discard the supernatant. Add 1 mL of TRIzol and 200 μL of chloroform to resuspend the cell pellet. Transfer the cell suspension to a 1.5 mL centrifuge tube and vigorously shake for 15 seconds. Let it stand at room temperature for 3 minutes. Pre-cool the centrifuge in advance, and centrifuge at 4°C, 12000 rpm for 20-30 minutes. After the centrifugation, aspirate 400-500 μL of the upper RNA aqueous phase, add an equal volume of isopropanol and mix thoroughly. Let it stand at room temperature for 10 minutes. Centrifuge at 4°C, 12000 rpm for 10 minutes, and form a white RNA precipitate at the bottom of the tube. Discard the supernatant. Add 1 mL of 75% ethanol, centrifuge at 4°C, 7500 rpm, 5 minutes to wash the RNA precipitate. Repeat this twice. After the washing is completed, discard the ethanol and open the cover of the ultracentrifuge to dry the RNA precipitate (when the RNA precipitate is transparent, it is ready). After drying, add 20 μL of DEPC-treated water to fully dissolve the RNA. Use a NanoDrop micro-volume spectrophotometer to detect the RNA concentration and record it for subsequent experiments.

1.6 Reverse Transcription

Prepare a 20 μL reverse transcription reaction mixture, which contains 4 μL of 5× All-In-One RT Master Mix, 1000 ng of total RNA, and the remaining volume is completed with DEPC-treated water. Place the prepared reaction mixture in the PCR machine, incubate at 37°C for 15 minutes to synthesize single-stranded cDNA; heat inactivate the reverse transcriptase at 85°C for 5 seconds; hold at 4°C for cooling. Detect the concentration of cDNA using a NanoDrop micro-volume spectrophotometer and record the results. Store the samples at -80°C for long-term storage and future use.

1.7 Primer Selection and RT-qPCR

Use the NCBI database to search for the gene sequence number, and look up the primers in PrimerBank. The sequences of the relevant gene primers for this experiment are as follows:

Table 3. Primer sequences.

Target	Primer	Sequence (5′–3′)
GAPDH	Forward	TGTTGCCATCAATGACCCCTT
GAPDH	Reverse	CTCCACGACGTACTCAGCG
CS	Forward	AACTGCTACCCAAGGCTAAGG
CS	Reverse	CTTTTGAGAGCCAAGATACCTGT
AMPKα1 (*PRKAA1*)	Forward	TTGAAACCTGAAAATGTCCTGCT
AMPKα1 (*PRKAA1*)	Reverse	GGTGAGCCACAACTTGTTCTT
ACC1 (*ACACA*)	Forward	ATGTCTGGCTTGCACCTAGTA
ACC1 (*ACACA*)	Reverse	CCCCAAAGCGAGTAACAAATTCT

Prepare a 10 μL qPCR reaction system, which contains 5 μL of 2×RealStar Power SYBR qPCR Mix, 2000 ng of cDNA template, 1 μL of primer mixture solution, and the remaining volume is filled with DEPC-treated water. The experiment sets up the NF group and the CAF group, and each group has 3 replicates. The qPCR reaction program is set as follows: 95℃ for denaturation (denaturation), 60℃ for annealing (primer binding), 72℃ for extension (DNA amplification), and the total reaction time is 90 minutes. After the reaction, collect the Ct values of each sample for subsequent data analysis.

1.8 Protein Extraction

Remove the culture medium and invert the culture dish onto a piece of absorbent paper to allow the absorbent paper to absorb the culture medium. Alternatively, place the culture dish upright to allow the remaining culture medium to flow to one side. Use a pipette to aspirate the medium. Add 3 mL of 4°C pre-cooled PBS to the culture dish and gently shake it for 1 minute to wash the cells. Discard the wash solution and repeat this process 3 times. After drying the PBS, place the culture dish on ice. Mix PMSF thoroughly to remove any crystals. Add 1 μL of PMSF (100×) and 1 μL of Cocktail (100×) to each 1 mL of the lysis solution and mix well before placing it on ice. In a 100 mm culture dish, add 400-600 μL of the lysis solution and place it on ice to lysate for 30 minutes. Shake it back and forth during the process to ensure the cells are fully lysed. After the lysis is complete, quickly scrape the cells onto one side of the culture dish using a clean cell scraper. Use a pipette to transfer the cell debris and lysis solution to a 1.5 mL centrifuge tube. Perform all the operations on ice as much as possible. Pre-cool the centrifuge, set it at 4°C and 12000 rpm to centrifuge the cell mixture for 30 minutes. Use a pipette tip to pick up the DNA sediment. If it is to be used in the short term, aliquot the supernatant into 0.5 mL centrifuge tubes and store them in a -20°C refrigerator. If it is to be used for a long term, transfer the supernatant to a new 1.5 mL centrifuge tube and store it in a -80°C refrigerator.

1.9 Protein Quantification by the BCA Assay

Precisely weigh 5mg of BSA standard substance, add 1mL of PBS buffer solution to fully dissolve and mix it, and prepare the BSA standard mother solution. Use the dilution method in multiples to prepare standard curve samples, setting the concentration gradient as 1000μg/mL, 500μg/mL, 250μg/mL, 125μg/mL, 62.5μg/mL, 31.25μg/mL, 15.625μg/mL and the blank control group (0μg/mL). Add 20μL of the corresponding concentration standard solution to each well. The protein sample to be tested is diluted 10 times with PBS, and 20μL is added to each well. Prepare an appropriate amount of BCA working solution according to the volume ratio of reagent A to reagent B of 50:1, mix well, and add 200μL of the BCA working solution to each well. Cover the plate with a plastic film and incubate it in a 37℃ constant temperature box in the dark for 30 minutes. Use the microplate reader to detect the absorbance (OD value) of each well at a wavelength of 562nm. Draw the standard curve by plotting the protein standard concentration as the abscissa and the corresponding absorbance as the ordinate. Calculate the sample concentration based on the absorbance of the test sample combined with the standard curve, and multiply by the dilution factor of the sample to obtain the actual concentration of the sample.

1.10 Western Blotting

Add an appropriate amount of 5× protein loading buffer to the protein sample, mix well, and then place it in a 95℃ metal bath for 10 minutes to fully denature the protein. Use SDS-PAGE gel electrophoresis to separate the protein. First, perform constant voltage electrophoresis at 80V for 30 minutes. After the sample enters the separating gel, adjust the voltage to 120V and continue electrophoresis for 60-90 minutes. The loading amount for each well is 30 μg of protein sample, and 5 μL of protein Marker is added to each well as a molecular weight reference. Before transferring the membrane, immerse the 0.45 μm PVDF membrane in anhydrous ethanol for 30 seconds to activate it. Use the wet transfer method, with a constant voltage of 100V, for 70 minutes to transfer the protein in the gel to the PVDF membrane. After the transfer is completed, place the PVDF membrane in a PBS-T buffer (containing 0.1% Tween-20) with 3% BSA, and incubate it at room temperature on a shaking table at 50 rpm for 1 hour. Discard the blocking solution, add the corresponding primary antibody diluent, and incubate it in a 4℃ refrigerator overnight. After the incubation is complete, wash the membrane 5 times with PBS-T buffer, each time for 5 minutes, at a shaking speed of 100 rpm. After the washing is completed, add 1:5000 diluted secondary antibody, incubate it at room temperature on a shaking table at 50 rpm for 1.5 hours. Again, use PBS-T buffer to wash the membrane 5 times, each time for 5 minutes, at a shaking speed of 100 rpm. Add ECL chemiluminescence developing solution, incubate in the dark for 4 minutes, and then expose for imaging. In this experiment, GAPDH is used as the internal reference protein. The dilution ratios of each antibody are as follows: GAPDH primary antibody 1:8000, AMPK primary antibody 1:2000, p-AMPK primary antibody 1:1000, ACC1 primary antibody 1:2000, p-ACC1 primary antibody 1:5000; all primary and secondary antibodies are diluted in PBS-T buffer (containing 0.1% Tween-20) containing 3% BSA. The dilutions are listed in Table 4.

Table 4. Antibody dilutions for western blotting.

Antibody	Dilution
GAPDH	1:8,000
AMPK (PRKAA1)	1:2,000
Phospho-AMPK	1:1,000
ACC1	1:2,000
Phospho-ACC1	1:5,000
HRP-conjugated anti-rabbit secondary antibody	1:5,000

1.11 Data Processing

1.11.1 RT-qPCR

The Ct values obtained from qPCR were calculated using the $2^{-\triangle\triangle Ct}$ method.

Control group: Subtract the mean Ct value of the 3 samples of the target gene in the NF group from the 3 samples of GAPDH in the NF group to obtain the first △ value (△Ct). Then, calculate the mean of the 3 differences to obtain the mean of ΔCt. Subtract the mean ΔCt from the 3 samples of the target gene in the NF group to obtain the second Δ value (Δ△Ct). Finally, calculate $2^{-\triangle\triangle Ct}$ for the 3 Ct values to obtain the results for the NF group.

Experimental group: Subtract the mean Ct value of the 3 samples of the target gene in the CAF group from the 3 samples of GAPDH in the CAF group to obtain the first △ value (△Ct). Subtract the mean ΔCt of the 3 samples of the target gene in the CAF group from the △Ct of the NF group to obtain the second Δ value (△△Ct). Finally, calculate $2^{-\triangle\triangle Ct}$ for the 3 Ct values to obtain the results for the CAF group.

1.11.2 Western Blotting

The protein band gray values were quantitatively detected using the ImageJ image analysis software, and the same detection area was uniformly selected for analysis. The gray values of each target protein band in the NF group and the CAF group were normalized and corrected by averaging with the corresponding internal reference GAPDH gray value. The relative expression levels of each target protein were calculated.

1.12 Statistical Analysis

All the experimental data in this study were statistically analyzed and graphically presented using GraphPad Prism 9. The data were expressed as "mean ± standard deviation". The comparison between the two groups was conducted using the independent sample t-test, and a difference was considered statistically significant when $P < 0.05$.

2 Results and Analysis

2.1 CAF Inhibits Fatty Acid Synthesis by Activating AMPK

To investigate the energy sources in CAF, Western Blot was used to detect the protein expressions of p-AMPK and p-ACC1 in CAF. The results showed that compared with NF, the protein expressions of p-AMPK and p-ACC1 in CAF significantly increased. Based on these results, the increase in the AMP/ATP ratio leads to the phosphorylation and activation of AMPK, which in turn phosphorylates ACC1 and inhibits its enzymatic activity, reducing the level of ACC1's fatty acid synthesis metabolism. When the fatty acid synthesis metabolism level decreases, CAF consumes the stored fatty acids in the body to make up for the energy gap caused by the low ATP level.

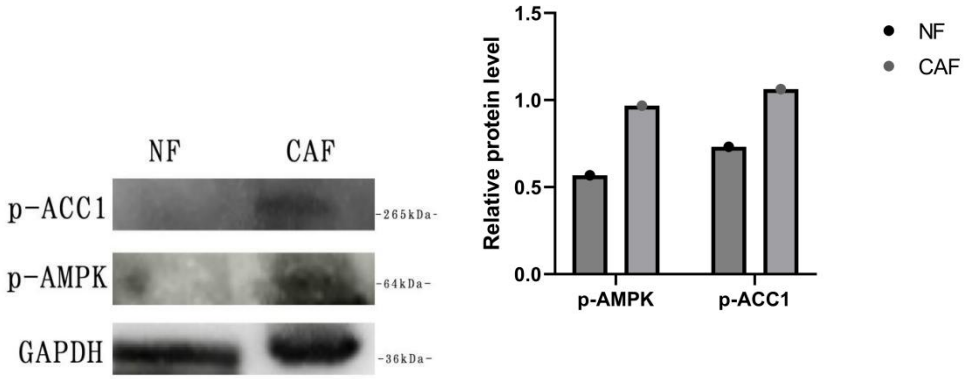


Fig. 1 The left panel shows the protein levels of p-AMPK, p-ACC1, and GAPDH in pancreatic cancer-associated fibroblasts and normal fibroblasts. The right panel presents the relative protein levels after normalization using the internal reference protein GAPDH.

2.2 CAF Experiences Prolonged Insufficient Energy Supply

To investigate the ATP level in CAF, the AMPK was detected by qPCR and Western Blot. The results showed that compared with NF, the mRNA and protein expression levels of AMPK in CAF significantly increased, indicating that CAF was in a long-term energy stress state. The prolonged abnormal increase in the AMP/ATP ratio led to the phosphorylation of AMPK, activation of downstream transcription factors, and an increase in the transcriptional level of AMPK.

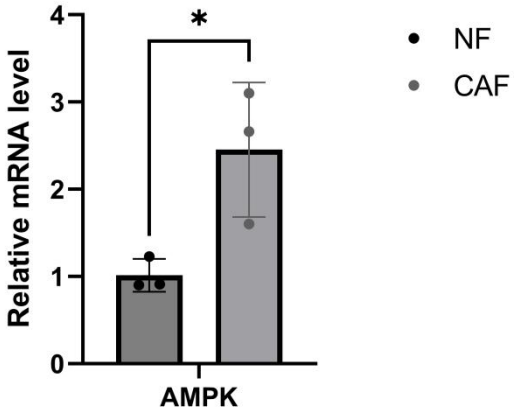


Fig. 2 Expression levels of AMPK mRNA in pancreatic cancer-associated fibroblasts. RNA was extracted from both cell types when the cell density reached 80%. The growth rates were similar. Normalization was performed using the reference gene GAPDH. The experiment was repeated three times, and t-test was used to analyze significance. *p<0.05.

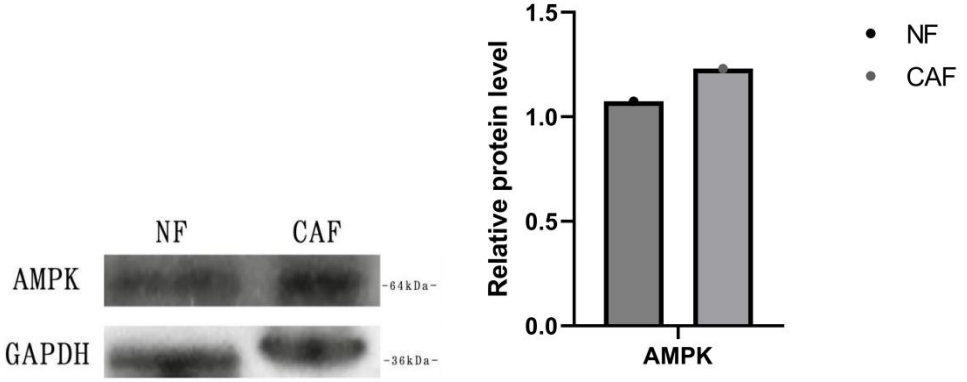


Fig. 3 The left panel shows the protein levels of AMPK and GAPDH in pancreatic cancer-associated fibroblasts and normal fibroblasts. The right panel presents the relative protein levels after normalization using the reference protein GAPDH.

2.3 High Expression of ACC1 in CAF

To further explore the characteristics of CAF cells, the expression levels of ACC1 downstream of AMPK were detected by qPCR and Western Blot. The results showed that compared with NF, the mRNA and protein expressions of ACC1 in CAF significantly increased. Thus, it can be concluded that CAF has a higher energy demand than NF.

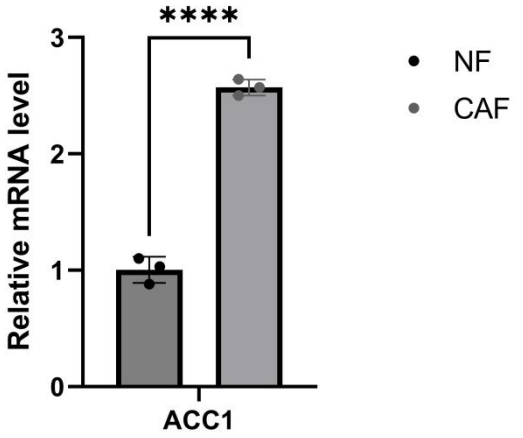


Fig. 4 Expression level of ACC1 mRNA in pancreatic cancer-associated fibroblasts. RNA was extracted from both cell types when the cell density reached 80%, and the growth rates were similar. Normalization was performed using the reference gene GAPDH. The experiment was repeated three times, and t-test was used to analyze the significance. ****$p < 0.0001$.

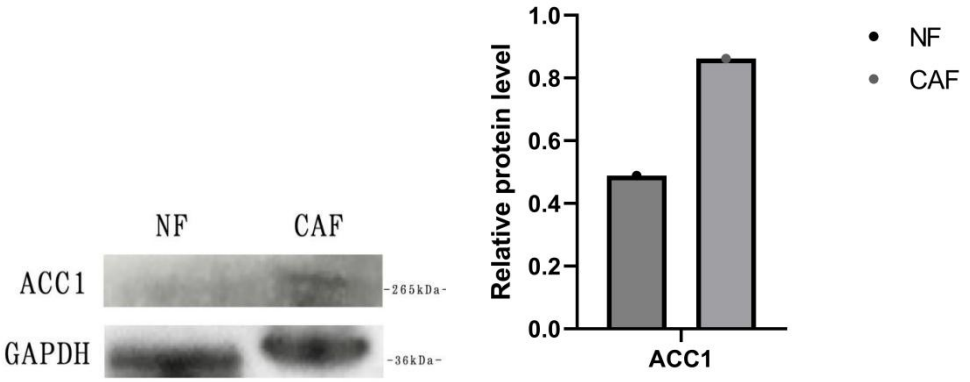


Fig. 5 The left figure shows the protein levels of ACC1 and GAPDH in pancreatic cancer-associated fibroblasts and normal fibroblasts. The right figure presents the relative protein levels after normalization using the internal reference protein GAPDH.

3 Discussion

Globally, the threat posed by pancreatic cancer is escalating [8-9]. It progresses rapidly and has a high mortality rate, being known as the "King of Cancers". Currently, there is an increasing amount of research on pancreatic cancer cells [10-12], but there is relatively less research on the tumor microenvironment, especially on the direction of metabolic reprogramming. Developing research and treatment targets from the perspective of energy supply or metabolism still has a lot of room for development.

In previous experiments, it was found that AMPK is activated under conditions of energy deficiency [13-14]. However, this experiment discovered that the abnormal activation of the AMPK-ACC1 signaling pathway in pancreatic cancer-associated fibroblasts occurs under conditions of adequate nutrition, by increasing fatty acid breakdown metabolism, providing energy for CAFs. Through the results of Western Blot, it was found that phosphorylation of AMPK leads to phosphorylation of its downstream ACC1, inhibiting the activity of ACC1, causing the synthesis of fatty acids to slow down or even stop. Subsequent experiments will conduct siRNA interference to knock down the AMPK gene and observe whether the proliferation of pancreatic cancer-associated fibroblasts is affected, thereby providing a treatment target for pancreatic cancer. In addition, the reasons for the abnormal activation of AMPK in CAFs under energy-sufficient conditions will also be explored.

There are still certain limitations in the experiments. When performing Western Blot, no three repetitions were conducted to eliminate accidental situations, and it is impossible to completely determine whether the results are a general situation. In the subsequent experiments, the experiments will be repeated to further confirm the protein expression contents of AMPK, ACC1, p-AMPK, and p-ACC1. At the same time, this experiment did not detailize the specific subtypes of pancreatic cancer CAFs, and cannot guarantee that the drugs will be effective for all types of CAFs. CAFs themselves have high heterogeneity [15], and it is speculated that the cells cultured in this laboratory belong to the myCAFs subgroup.

References

[1] Sébastien Herzig, Reuben J Shaw. AMPK: guardian of metabolism and mitochondrial homeostasis, Nat Rev Mol Cell Biol, 2017, 19(2):121-135. doi:10.1038/nrm.2017.95.

[2] Hardie DG, Carling D, Gamblin SJ. AMP-activated protein kinase: also regulated by ADP, Trends Biochem Sci, 2011, 36:470-477. doi:10.1016/j.tibs.2011.06.004.

[3] Che-Chia Hsu, Danni Peng, Zhen Cai, Hui-Kuan Lin. AMPK signaling and its targeting in cancer progression and treatment, Semin Cancer Biol, 2022, 85:52-68. doi:10.1016/j.semcancer.2021.04.006.

[4] Jian A, Bai X, Yang N, Shen P. Effect and mechanism of acetyl-CoA carboxylase 1 in regulating the proliferation of hepatocellular carcinoma cells, J China Pharm Univ, 2024, 55(6):783-794. doi:10.11665/j.issn.1000-5048.2024032002.

[5] Witters LA, Nordlund AC, Marshall L. Regulation of intracellular acetyl-CoA carboxylase by ATP depletors mimics the action of the 5'-AMP-activated protein kinase, Biochem Biophys Res Commun, 1991, 181(3):1486-1492.

[6] Yiming Guo, Nuo Xu, Qinyu Meng. Mechanisms of Inonotus obliquus (Fr.) Pilát polysaccharides in ameliorating lipid-induced skeletal muscle insulin resistance via PI3K/AKT and AMPK/ACC1/CPT1 signaling pathways, J Ethnopharmacol, 2025, 349:119938. doi:10.1016/j.jep.2025.119938.

[7] Huang R, Guo F, Li Y, Liang Y, Li G, Fu P, Ma L. Activation of AMPK by triptolide alleviates nonalcoholic fatty liver disease by improving hepatic lipid metabolism, inflammation and fibrosis, Phytomedicine, 2021, 92:153739. doi:10.1016/j.phymed.2021.153739.

[8] Julia Mayerle, Matthias Sendler, Eszter Hegyi. Genetics and pathophysiology of pancreatitis, Gastroenterology, 2019, 156(7):1951-1968.e1. doi:10.1053/j.gastro.2018.11.081.

[9] Alison P Klein. Pancreatic cancer epidemiology: understanding the role of lifestyle and inherited risk factors, Nat Rev Gastroenterol Hepatol, 2021, 18(7):493-502. doi:10.1038/s41575-021-00457-x.

[10] Della Corte C, Faraci S, Majo F, Lucidi V. Pancreatic disorders in children: New clues on the horizon, Dig Liver Dis, 2018. doi:10.1016/j.dld.2018.06.016.

[11] Mayerle J, Sendler M, Hegyi E. Genetics, Cell Biology, and Pathophysiology of Pancreatitis, Gastroenterology, 2019, 156(7):1951-1968.e1. doi:10.1053/j.gastro.2018.11.081.

[12] Rana SS. An overview of walled-off pancreatic necrosis for clinicians, Expert Rev Gastroenterol Hepatol, 2019, 13(4):331-343. doi:10.1080/17474124.2019.1574568.

[13] Mao KS, Li MS, Zhou J. Update on the roles of liver kinase B1 in pancreatic cancer, Shijie Huaren Xiaohua Zazhi, 2015, 23(19):3086-3093. doi:10.11569/wcjd.v23.i19.3086.

[14] Cheng WJ, Cheng JD, Jing XB. AMPK and gastrointestinal carcinoma, Shijie Huaren Xiaohua Zazhi, 2012, 20(4):304-309. doi:10.11569/wcjd.v20.i4.304.

[15] Niu N, Shen X,Tumor cell-intrinsic epigenetic dysregulation shapes cancer-associated fibroblasts heterogeneity to metabolically support pancreatic cancer.,Cancer Cell. 2024 May 13;42(5):869-884.e9. doi: 10.1016/j.ccell.2024.03.005.